Quasisteady Particle Transport in Slowly Varying Periodic Streaming Flows

Rodrigo Abrajan-Guerrero [*] **Jeff D. Eldredge** [**]
Stuart T. Smith [***] **Scott David Kelly** [****]

[*] *Department of Mechanical Engineering and Engineering Science, University of North Carolina at Charlotte, Charlotte, NC 28223-0001 USA (e-mail: rabrajan@uncc.edu)*
[**] *Department of Mechanical and Aerospace Engineering, University of California, Los Angeles, Los Angeles, CA 90095-1597 USA (e-mail: eldredge@seas.ucla.edu)*
[***] *Department of Mechanical Engineering and Engineering Science, University of North Carolina at Charlotte, Charlotte, NC 28223-0001 USA (e-mail: stusmith@uncc.edu)*
[****] *Department of Mechanical Engineering and Engineering Science, University of North Carolina at Charlotte, Charlotte, NC 28223-0001 USA (e-mail: scott@kellyfish.net)*

Abstract: When a cylindrical probe vibrates laterally in a fluid at a Reynolds number of order 10, a circulatory pattern of flow is established in the fluid near the probe. In a plane transverse to the probe, a symmetric arrangement of four streaming cells is maintained by the probe's vibration. A computational model has shown that inertial particles introduced to such a flow will be attracted to the centers of the streaming cells. We present preliminary experimental data supporting this prediction and outline a strategy whereby particles captured in this way can be transported from place to place as a result of periodic variations in the excitation of a fluid containing two independent probes. Specifically, we model the time-averaged flow around two probes by superposing two copies of a velocity field obtained analytically for the single-probe case and demonstrate that a cyclic change in the two-probe flow can engender acyclic variations in the positions and character of fixed points. A fixed point that's initially attractive to inertial particles can be moved from the vicinity of one probe to the vicinity of another and then annihilated or altered via bifurcation so that it will surrender the particles it carries. If parametric variations in such a flow are slow relative to the dynamics of particles migrating to attracting points, then the net displacement of inertial particles from one trapping point to another as a result of a cyclic change in the flow exhibits certain features of a geometric phase.

Keywords: nonlinear systems, differential geometric methods, flow control, parametric excitation, biomedical systems

1. INTRODUCTION

The ability to manipulate particles suspended in fluids on a micrometer scale has a variety of applications, some of which prohibit individual mechanical particle handling. The particles in question may be cells from a biological sample, to be separated according to cell type and tallied for cancer diagnosis (de Bono et al. (2008)), for instance, or they may be abrasive particles to be circulated in proximity to a brittle surface for precision machining (Nowakowski et al. (2009); Howard et al. (2013)). The first of these applications illustrates the need for contact-free technology to manipulate fragile particles without risking damage to them. Both examples illustrate the need for high-throughput technology that can direct the sustained transport of particles without feedback control at the level of individual particle position.

To collect nutrients from their surroundings, sessile aquatic protozoa like *Vorticella* use vibrating cilia to drive streaming flows that transport nearby food particles to their mouths (Vogel (2003)). Although a single such organism may possess many cilia, it's common for the cilia of a single organism to beat synchronously to drive a flow that can be characterized with relatively few parameters. Circulatory patterns like those observed near the mouth of a solitary feeding protozoan can even be established by exciting a fluid with a single vibrating probe. [1] If a fluid is excited by several probes vibrating independently in proximity to each other, complex patterns of material transport can be created and manipulated by varying the amplitudes, frequencies, and directions of the probes' motion. The authors believe that this suggests a practicable approach for particle manipulation in engineered environments.

⋆ Support for this work was provided in part by the National Science Foundation grant CMMI-1000656.

[1] Video footage of such an experiment, conducted by the third author, is visible at `http://kellyfish.net/insitutec.mov`. The probe in the video is roughly 6 μm thick.

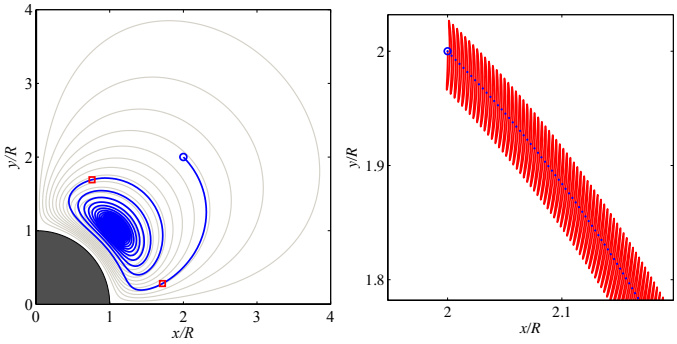

Fig. 1. *Left:* The time-averaged trajectory of a small inertial particle against the backdrop of time-averaged Lagrangian streamlines in a flow with Reynolds number 40, described in detail in Chong et al. (2013). *Right:* A portion of the particle's actual trajectory (in red) with periodic samples exhibiting net motion (in blue).

2. PARTICLE CAPTURE IN STREAMING FLOWS DRIVEN BY VIBRATING CYLINDERS

To better understand particle transport near a single laterally vibrating cylinder at Reynolds numbers of order 10, the authors recently developed a model based on an analytical representation (from Holtsmark et al. (1954)) of the flow near such a cylinder in the absence of particles. While the addition of particles of arbitrary size may perturb such a flow significantly, sufficiently small particles represent a negligible perturbation. This is the premise of the *Maxey-Riley equations* (from Maxey and Riley (1983)), which model the behavior of a small particle driven by a background flow by assuming that the flow dynamics are independent of the particle dynamics. In Chong et al. (2013), the authors and a collaborator used the Maxey-Riley equations to demonstrate that small particles suspended in the fluid near a single vibrating cylinder will be attracted to the centers of four streaming cells that persist at locations arranged symmetrically around the cylinder's average position.

Fig. 1 illustrates this trapping of particles. The left panel depicts the flow in one quadrant adjacent to the cylinder, which is shown in grey. The cylinder vibrates from left to right, and the flow shown is mirrored in the three omitted quadrants. Although the flow is unsteady, the time-averaged trajectories of fluid particles — the time-averaged *Lagrangian streamlines* — are closed. Some such streamlines are shown in light grey. Fluid particles complete excursions around these streamlines slowly; each oscillation in the cylinder's position advances a fluid particle a small distance (in the net) along one of these streamlines. The small material displacement of the fluid by each cyclic variation in its boundary is known as *Stokes drift*, having first been analyzed (in the context of a different physical problem) in Stokes (1847).

The right panel in Fig. 1 depicts (in red) a portion of the trajectory of an inertial particle driven by the background flow. This trajectory was computed by integrating the Maxey-Riley equations numerically. Since the fluid oscillates with the cylinder, so too does the particle, and the trajectory shown exhibits a significant high-frequency component. The net displacement of the particle after each oscillation is nonzero, however, and periodic sampling of the particle's position (in blue) reveals a distinct average trajectory. The blue spiral in the left panel represents a more extensive set of periodic samples from the particle's trajectory. The point on the blue spiral that's farthest from the cylinder is the particle's initial location; vibration of the cylinder induces the particle to migrate to the center of the innermost Lagrangian streamline.

3. PHYSICAL MODEL VALIDATION

Fig. 2 depicts an experimental apparatus that's been developed to verify the phenomenon of particle capture shown in Fig. 1. A cylindrical probe half a millimeter thick protrudes downward from an aluminum flexure (Smith (2000)) into a petri dish containing water seeded with silvered glass beads. The flexure is driven piezoelectrically to cause the probe to vibrate laterally at a frequency adjustable up to 10 kHz. A horizontal plane containing a cross section of the probe away from its tip is imaged with a high-speed video camera.

The left side of Fig. 3 depicts still frames from footage captured using the system in Fig. 2. Each of the four frames in the top row represents the superposition of its predecessors (from left to right) with a subsequent still image. Each of the four frames in the bottom row is a close-up of the top left corner of the frame above, as indicated by the yellow box. The vibrating probe is seen in the center of each frame in the top row and in the corner of each frame in the bottom row. The blue circular disk overlapping the bottom right frame indicates the position and scale of the probe and its direction of motion.

The experiment depicted in Fig. 3 is preliminary, but the images clearly show that glass beads in proximity to the probe, visible as light pixels, spiral inward toward the centers of the four surrounding streaming cells. The leftmost frame in the bottom row depicts beads distributed around a cell with an unpopulated center. Each subsequent frame indicates increased migration of beads into this center, highlighted by the yellow arrow in the third panel.

The right side of Fig. 3 reconstructs the time-averaged velocity field representing the beads' motion around one streaming cell via *particle image velocimetry*, inferring velocity vectors from comparisons of sequential still images. Again, the blue circular disk indicates the probe's scale and direction of motion. Because the beads used in this experiment are small and neutrally dense, their velocities resemble the velocities of fluid particles and their time-averaged trajectories diverge only gradually from time-averaged Lagrangian streamlines. Because the probe vibrates thousands of times per second, however, beads are captured in the centers of streaming cells within seconds.

4. CONTROL VIA GEOMETRIC PHASE

The concept of *geometric phase* applies when a cyclic change in some of the variables specifying a system's configuration engenders a net change in other such variables in a manner that's independent of time parametrization. Typically, the context is that of a system with a configuration manifold exhibiting a physically meaningful bundle structure. The configuration of a robotic vehicle that

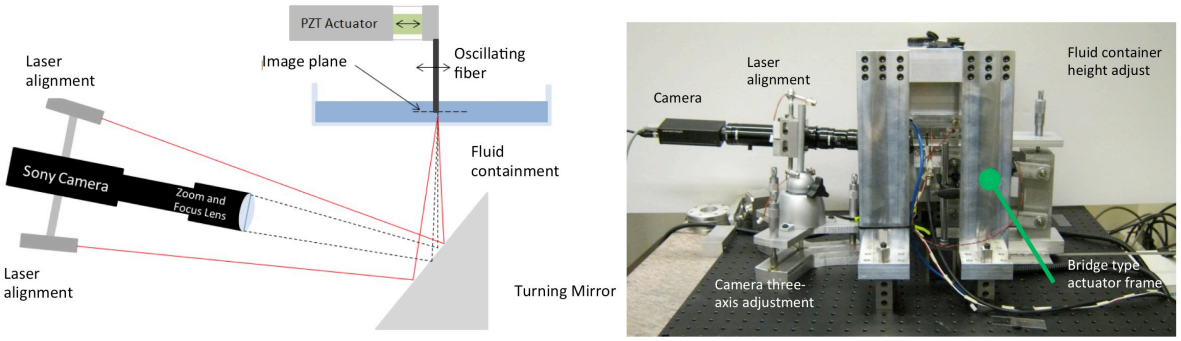

Fig. 2. Apparatus for imaging particle transport near a solitary vibrating probe.

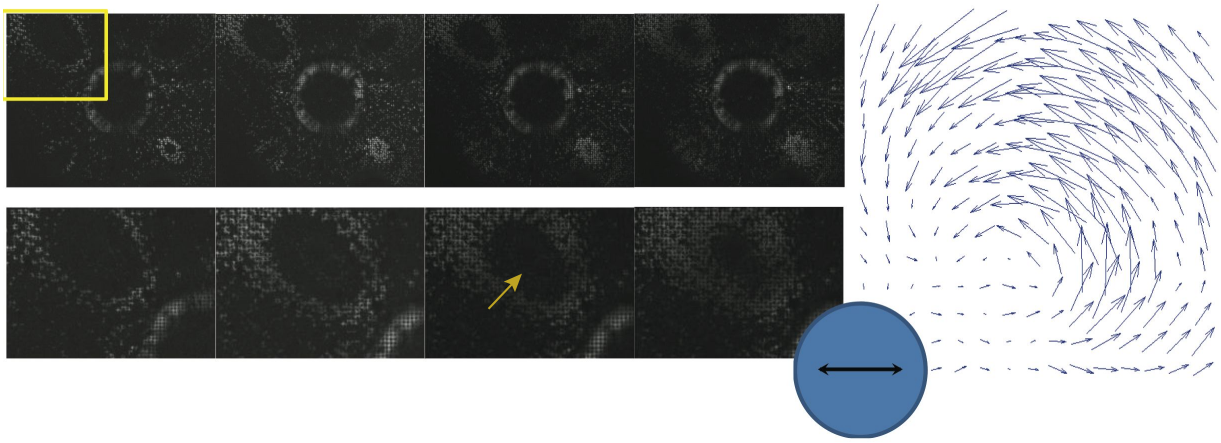

Fig. 3. *Left:* Superposed frames from video captured using the apparatus from Fig. 2, indicating particle capture consistent with Fig. 1. *Right:* Velocity field data reconstructed from comparisons of particle positions in successive frames. The blue probe is positioned to fit both sides of the figure.

changes its internal shape to propel itself, for instance, corresponds to a point in a bundle over the manifold of points representing internal shapes. Fibers of this bundle are copies of the Lie group of translations and/or rotations of the vehicle in ambient space; the net translation and/or rotation associated with a cyclic shape change — in other words, the net resulting fiberwise displacement — represents a geometric phase if it's independent of the rate at which this change is executed. Robotic locomotion based on geometric phase was discussed in detail in Kelly and Murray (1995).

Stokes drift provides another example of geometric phase. The deliberate displacement of fluid particles as a result of cyclic displacements in the position of a cylindrical probe was treated as a control problem in Or et al. (2009). The objective therein was the design of trajectories in the manifold of probe positions to generate desired fiberwise displacements in a symplectic bundle over this manifold. The evolution of a fluid surrounding a moving probe consists exclusively of geometric phase in the driftless Reynolds-number extremes of ideal flow and Stokes flow; the mathematical parallelism between these physically diverse settings was discussed in Kelly and Murray (1996).

In the present paper, we invoke the concept of geometric phase in the context of inertial particle transport near a pair of parallel probes like the probes in Figs. 1 and 3 vibrating independently in proximity to one another. The motion of each probe is parametrized by its axis, amplitude, and frequency of vibration. Each choice of these parameters determines a periodic flow characterized by a time-averaged Lagrangian streamline pattern akin to, but topologically more complex than, that in the left panel of Fig. 1. Inertial particles released into this flow will, over time, accumulate at trapping points corresponding to centers — or, presumably, to sufficiently stable spirals — in the averaged Lagrangian velocity field.

In general, if the parameters specifying the motion of the probes are varied gradually, trapping points in the flow will be displaced gradually, transporting trapped particles with them in a reversible manner. If flow parameters attain certain combinations of values, however, bifurcations in the averaged flow field may occur that cause trapping points to alter their character as fixed points or to vanish entirely. When a trapping point ceases to be attractive to inertial particles, the particles it carries will be released to converge to other trapping points. This process is irreversible; restoring a trapping point that's surrendered its particles won't recover these particles if they've been given time to settle at another trapping point.

Suppose that the parameters specifying the motion of the probes are varied in a cyclic manner, but that particles in the flow are given time at every step to converge to trapping points. If a cyclic excursion in parameter space induces no bifurcation in the time-averaged flow, then trapped particles will exhibit no net displacement at the end of each cycle. If a cycle involves one or more

bifurcations, however, particles trapped at a certain point at the beginning of the cycle may be trapped elsewhere at the end of the cycle, even though the original flow field has been restored. As long as the flow is deformed slowly relative to the migratory dynamics of untrapped particles, furthermore, the net transport of particles throughout the flow associated with a particular cyclic variation in parameters will depend only on the geometry of the loop executed in parameter space and not on its time parametrization.

In this last regard, the net transport of inertial particles associated with a slow cyclic deformation of the flow resembles the geometric phase associated with a closed path in a manifold on which coordinates correspond to directions, amplitudes, and frequencies of probe vibration. This phase corresponds to fiberwise motion within a bundle over the aforementioned manifold; points in each fiber correspond to arrangements of trapped particles within the flow. We defer a deeper analysis of this interpretation for another paper, but we demonstrate explicitly in Section 5 that cyclic parametric variations can indeed produce bifurcations of the kind required for net particle transport.

5. TRANSPORT OF CAPTURED PARTICLES VIA PERIODIC FLOW DEFORMATION

The Lagrangian streamline pattern depicted in the left panel of Fig. 1 is based on an analytical expression obtained in Holtsmark et al. (1954). A simplified model for the same time-averaged flow field, limited in scope to the flow outside a thin boundary layer surrounding the cylinder, was developed in Schlichting (1932), where versions of the velocity field were obtained for the case in which no outer boundary is present and for the case in which a circular outer boundary is present.

In the present paper, we model the flow transverse to a pair of vibrating probes by superposing two copies of the bounded velocity field from Schlichting (1932), each parametrized to match the excitation due to one of the probes. This model is clearly an approximation, since the velocity field associated with either probe will fail to satisfy the boundary conditions on the other probe, and since the outer circular boundaries observed by the two individual fields will be misaligned. Sufficiently far from boundaries, however, we believe our model to represent the correct averaged velocity field with sufficient fidelity to warrant analysis.

Schlichting (1932) considered the flow around a transversely vibrating cylinder of radius r_1 enclosed by a circular boundary of radius R. The stream function Ψ is given in polar coordinates (r, ϕ) by

$$\Psi = A\left(\frac{C_1}{r^2} + C_2 + C_3 r^2 + C_4 r^4\right)\sin(2\phi) \qquad (1)$$

with

$$A = -\frac{3}{2}\frac{s^2\omega}{r_1},$$

where s and ω are the magnitude and angular velocity of the oscillations, respectively. The boundary conditions are

$$-\frac{1}{r}\frac{\partial\Psi}{\partial\phi} = v_r = 0$$

on the bounding walls,

$$\frac{\partial\Psi}{\partial r} = v_\phi = A\sin(2\phi)$$

for $r = r_1$, and

$$v_\phi = 0$$

for $r = R$. For more details see Schlichting (1932).

Applying these boundary conditions, we can solve for the coefficients in (1) to obtain

$$C_1 = -\frac{R^4 r_1^3}{2\left(R^2 - r_1^2\right)^2},$$
$$C_2 = \frac{r_1\left(R^4 + 2R^2 r_1^2\right)}{2\left(-R^2 + r_1^2\right)^2},$$
$$C_3 = -\frac{r_1\left(2R^2 + r_1^2\right)}{2\left(R^2 - r_1^2\right)^2},$$
$$C_4 = \frac{r_1}{2\left(-R^2 + r_1^2\right)^2}.$$

The velocity field is given in polar coordinates by

$$v_r = \frac{3s^2\omega\left(r^2 - R^2\right)^2\left(r^2 - r_1^2\right)\cos(2\phi)}{2r^3\left(R^2 - r_1^2\right)^2},$$
$$v_\phi = \frac{3s^2\omega\sin(\phi)\cos(\phi)\left(-2r^6 + r^4\left(2R^2 + r_1^2\right) - R^4 r_1^2\right)}{r^3\left(R^2 - r_1^2\right)^2}$$

and in Cartesian coordinates by

$$\begin{aligned}\dot{x} =& \frac{3s^2\omega\, x}{2\left(R^2 - r_1^2\right)^2}\left[\frac{\left(r_{\mathrm{xy}}^2 - r_1^2\right)\left(x^2 - y^2\right)\left(r_{\mathrm{xy}}^2 - R^2\right)^2}{\left(r_{\mathrm{xy}}^2\right)^3}\right.\\ &\left. + \frac{2y^2\left(R^2 - r_{\mathrm{xy}}^2\right)\left(r_1^2 R^2 + r_{\mathrm{xy}}^2\left(r_1^2 - 2r_{\mathrm{xy}}^2\right)\right)}{\left(r_{\mathrm{xy}}^2\right)^{5/2}}\right],\\ \dot{y} =& \frac{3s^2\omega\, y}{2\left(R^2 - r_1^2\right)^2}\left[\frac{\left(r_{\mathrm{xy}}^2 - r_1^2\right)\left(x^2 - y^2\right)\left(r_{\mathrm{xy}}^2 - R^2\right)^2}{\left(r_{\mathrm{xy}}^2\right)^3}\right.\\ &\left. - \frac{2x^2\left(R^2 - r_{\mathrm{xy}}^2\right)\left(r_1^2 R^2 + r_{\mathrm{xy}}^2\left(r_1^2 - 2r_{\mathrm{xy}}^2\right)\right)}{\left(r_{\mathrm{xy}}^2\right)^{5/2}}\right],\end{aligned} \qquad (2)$$

where

$$r_{xy}^2 = x^2 + y^2.$$

We can use (2) to plot the average streamlines that result from the vibrations of the cylinder; such a plot is shown in Fig. 4. The stream plot shows four symmetric streaming cells. The four fixed points are linear centers, which implies that (according to Chong et al. (2013)) particles would be attracted to these locations. The positions of these fixed points depend only on the radii r_1 and R. The coordinates of the fixed points are (x_c, y_c), with

$$x_c = \pm\frac{\sqrt{\sqrt{\mathrm{r1}^2\left(8R^2 + \mathrm{r1}^2\right)} + \mathrm{r1}^2}}{2\sqrt{2}},$$
$$y_c = \pm\frac{\sqrt{\sqrt{\mathrm{r1}^2\left(8R^2 + \mathrm{r1}^2\right)} + \mathrm{r1}^2}}{2\sqrt{2}}.$$

The model with two vibrating cylinders is constructed by superposing the vector fields induced by two independent cylinders. To each cylinder we assign a parameter θ representing the angle between the direction of oscillation and

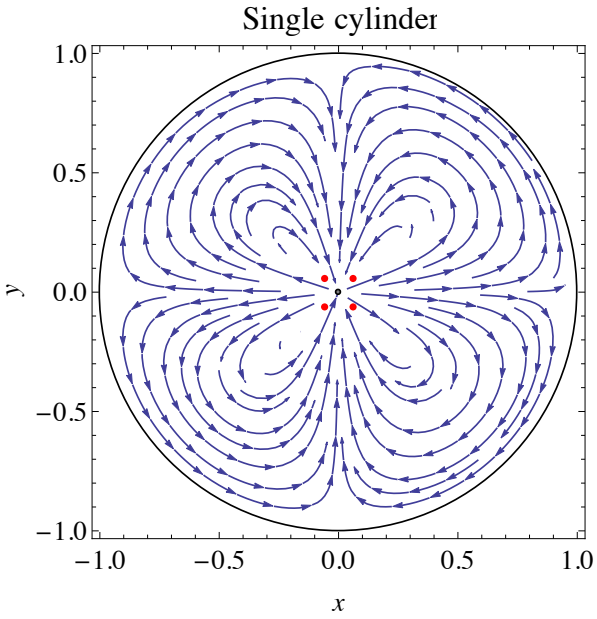

Fig. 4. Streamlines generated by a solitary vibrating cylinder. Motion of the cylinder is parallel to the x-axis. The cylinder is indicated by the tiny grey disk in the center of the figure; the outer boundary of the region has a much larger radius than the cylinder in order to approximate the conditions of experiments like that shown in Fig 3. The four red dots represent the positions of fixed points in the velocity field. The parameters used to generate this plot were $s = 0.009$, $\omega = 3.1$, $r_1 = 0.01$, and $R = 1$.

the x-axis and an additional pair of parameters representing the cylinder's displacement from the origin.

The procedure to rotate and translate a cylinder (and the velocity field it generates) is as follows. If

$$\dot{x} = f(x, y), \qquad \dot{y} = g(x, y)$$

denote the velocity field given by (2) and $\mathfrak{R}(\theta)$ is a rotation matrix

$$\mathfrak{R}(\theta) = \begin{bmatrix} \cos\theta & -\sin\theta \\ \cos\theta & \sin\theta \end{bmatrix},$$

then the vector field rotated by the angle θ will be given by

$$\begin{bmatrix} \tilde{f}(x, y, \theta) \\ \tilde{g}(x, y, \theta) \end{bmatrix} = \mathfrak{R}(\theta) \begin{bmatrix} f(\mathfrak{R}(-\theta)[x, y]^T) \\ g(\mathfrak{R}(-\theta)[x, y]^T) \end{bmatrix}.$$

For translation from the origin to the point (h, k), we define the map

$$\mathfrak{T} : \begin{bmatrix} \tilde{f}(x, y) \\ \tilde{g}(x, y) \end{bmatrix} \mapsto \begin{bmatrix} \tilde{f}(x - h, y - k, \theta) \\ \tilde{g}(x - h, y - k, \theta) \end{bmatrix};$$

the rotated and translated vector field is given by

$$\begin{bmatrix} \dot{x} \\ \dot{y} \end{bmatrix} = \begin{bmatrix} \tilde{f}(x - h, y - k, \theta) \\ \tilde{g}(x - h, y - k, \theta) \end{bmatrix}. \tag{3}$$

We now consider the specific case of two cylinders, separated symmetrically along the x axis by a distance 0.3, with angles θ_1 and θ_2. This vector field can be obtained by the direct addition of two vector fields of the form (3), yielding

$$\begin{bmatrix} \dot{x} \\ \dot{y} \end{bmatrix} = \begin{bmatrix} \tilde{f}(x - h_1, y - k_1, \theta_1) + \tilde{f}(x - h_2, y - k_2, \theta_2) \\ \tilde{g}(x - h_1, y - k_1, \theta_1) + \tilde{g}(x - h_2, y - k_2, \theta_2) \end{bmatrix}$$

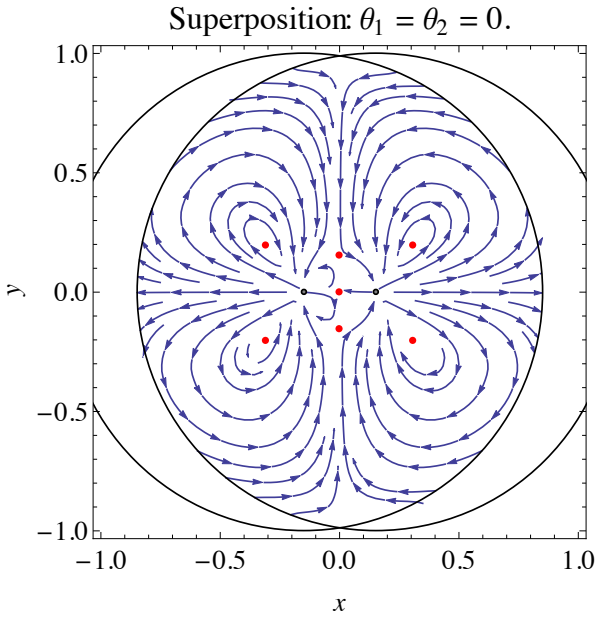

Fig. 5. Superposition of two velocity fields created by the vibration of two cylinders with spacing of 0.3. Only the intersection of the two circular regions with radius R centered around the two cylinders is shown. (Axis labels will be omitted in further plots.)

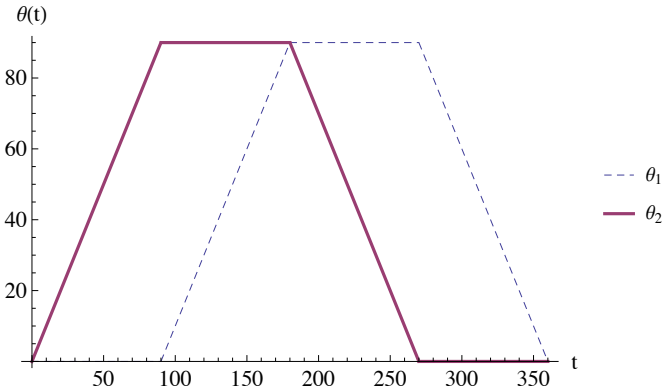

Fig. 6. Time parametrization of θ_1 and θ_2.

with $h_1 = -0.15$, $h_2 = 0.15$, and $k_1 = k_2 = 0$. A stream plot for this field with $\theta_1 = \theta_2 = 0$ can be seen in Fig. 5.

We next apply a cyclic variation to the control parameters θ_1 and θ_2, parametrized in degrees as

$$\theta_1(t) = \begin{cases} 0 & 0 \le t \le 90 \\ t - 90 & 90 \le t \le 180 \\ 90 & 180 \le t \le 270 \\ -t + 360 & 270 \le t \le 360 \end{cases},$$
$$\theta_2(t) = \begin{cases} t & 0 \le t \le 90 \\ 90 & 90 \le t \le 180 \\ -t + 270 & 180 \le t \le 270 \\ 0 & 270 \le t \le 360 \end{cases}. \tag{4}$$

These functions are plotted against time in Fig. 6. In Fig. 7 we show a sequence of snapshots of the velocity field generated by the vibrating cylinders as θ_1 and θ_2 vary. For $\theta_1 = \theta_2 = 0$, the velocity field is the same as that shown in Fig. 5. We track the trajectory of one fixed point, shown as a dot in the top left panel of Fig. 7, in pink.

From $t = 0$ to $t = 180$, this fixed point moves smoothly from right to left, interacting closely with no other fixed point. At $t = 90$, the fixed point is clearly a center. From $t = 180$ to $t = 268$, the fixed point and a saddle point approach each other. Right after $t = 268$, approximately when $\theta_1 = 1.7°$ and $\theta_2 = 90°$, a collision occurs in which the fixed point we've been tracking is annihilated.

Another bifurcation occurs shortly thereafter, when $t \approx 276$, and a new saddle point and spiral emerge nearby. These are seen as dots in the third panel in the middle row of Fig. 7; we now track their trajectories in pink. The spiral follows a trajectory thereafter that leads it to collide with another saddle and vanish shortly after $t = 312$. The saddle point survives the completion of the cyclic variation in θ_1 and θ_2, migrating to the location of one of the saddles that were visible at the beginning of the cycle.

This example represents only one of many cyclic variations that can be applied to the excitation of a pair of vibrating cylindrical probes, but it illustrates that such a cyclic variation can induce a fixed point that's initially attractive to inertial particles to migrate significantly from its initial location in the flow and then to vanish, releasing whatever particles it carried with it into the basin of attraction of a different fixed point. Though inducing no net change in the fluid velocity field, a cyclic change in flow parameters can thus result in the net redistribution of trapped inertial particles in the neighborhood of a pair of probes.

ACKNOWLEDGEMENTS

The authors thank Kwitae Chong for computational work depicted in Fig. 1 and Stephen Howard, Eric Fleischhauer, and Phanindra Tallapragada for experimental work depicted in Figs. 2 and 3.

REFERENCES

Chong, K., Kelly, S.D., Smith, S.T., and Eldredge, J.D. (2013). Inertial particle trapping in viscous streaming. *Physics of Fluids*, 25(033602).

de Bono, J.S., Scher, H.I., Montgomery, R.B., Parker, C., Miller, M.C., Tissing, H., Doyle, G.V., Terstappen, L.W.W.M., Pienta, K.J., and Raghavan, D. (2008). Circulating tumor cells predict survival benefit from treatment in metastatic castration-resistant prostate cancer. *Clinical Cancer Research*, 14, 6302–6309.

Holtsmark, J., Johnsen, I., Sikkeland, T., and Skavlem, S. (1954). Boundary layer flow near a cylindrical obstacle in an oscillating, incompressible fluid. *Journal of the Acoustical Society of America*, 26(1), 26–39.

Howard, S.C., Chesna, J.W., Smith, S.T., and Mullany, B.A. (2013). An apparatus for vortex machining studies. *Journal of Manufactuing Science and Engineering*, 135, 051005.

Kelly, S.D. and Murray, R.M. (1995). Geometric phases and robotic locomotion. *Journal of Robotic Systems*, 12, 417–431.

Kelly, S.D. and Murray, R.M. (1996). The geometry and control of dissipative systems. In *Proceedings of the 35th IEEE Conference on Decision and Control*.

Maxey, M.R. and Riley, J.J. (1983). Equation of motion of a small rigid sphere in a non-uniform flow. *Physics of Fluids*, 26, 883–889.

Nowakowski, B., Smith, S.T., Mullany, B.D., and Woody, S.C. (2009). Vortex machining: Localized surface modification using an oscillating fiber probe. *Machining Science and Technology*, 13, 561–570.

Or, Y., Vankerschaver, J., Kelly, S.D., Murray, R.M., and Marsden, J.E. (2009). Geometric control of particle manipulation in a two-dimensional fluid. In *Proceedings of the 48th IEEE Conference on Decision and Control & 28th Chinese Control Conference*.

Schlichting, H. (1932). Berechnung ebener periodischer grenzschichtströmungen. *Physikalische Zeitung*, 33, 327–335.

Smith, S.T. (2000). *Flexures: Elements of Elastic Mechanisms*. Gordon and Breach.

Stokes, G.G. (1847). On the theory of oscillatory waves. *Transactions of the Cambridge Philosophical Society*, 8, 441–455.

Vogel, S. (2003). *Comparative Biomechanics: Life's Physical World*. Princeton University Press.

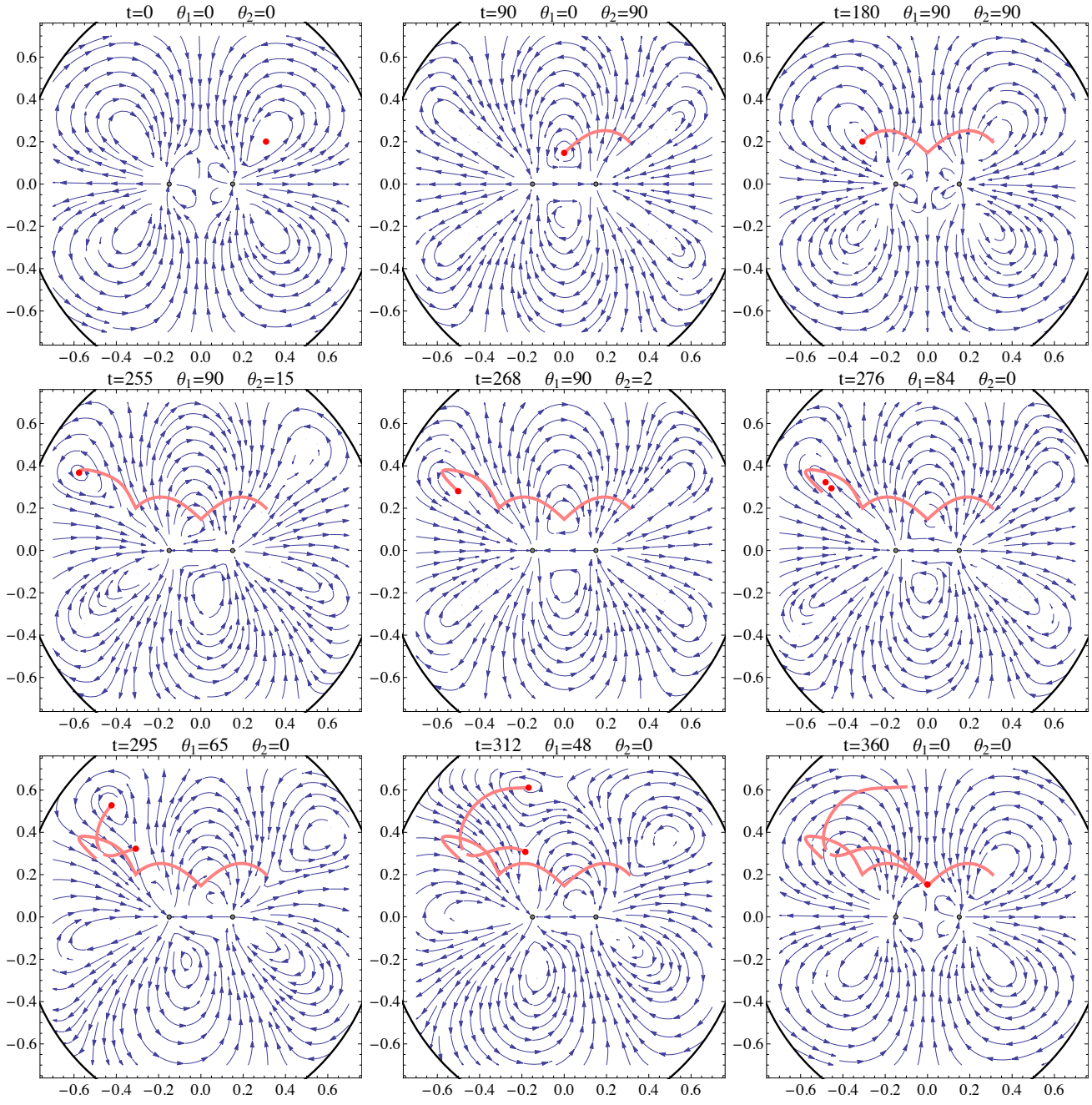

Fig. 7. Sequence of stream plots generated as θ_1 and θ_2 vary through one cycle according to (4). The sequence goes from left to right, then from top to bottom.